

**Исследование вклада атлантических и  
тихоокеанских вод в процесс сокращения  
арктического морского льда**

**Е.Н. Голубева, Д.Ф.Якшина**

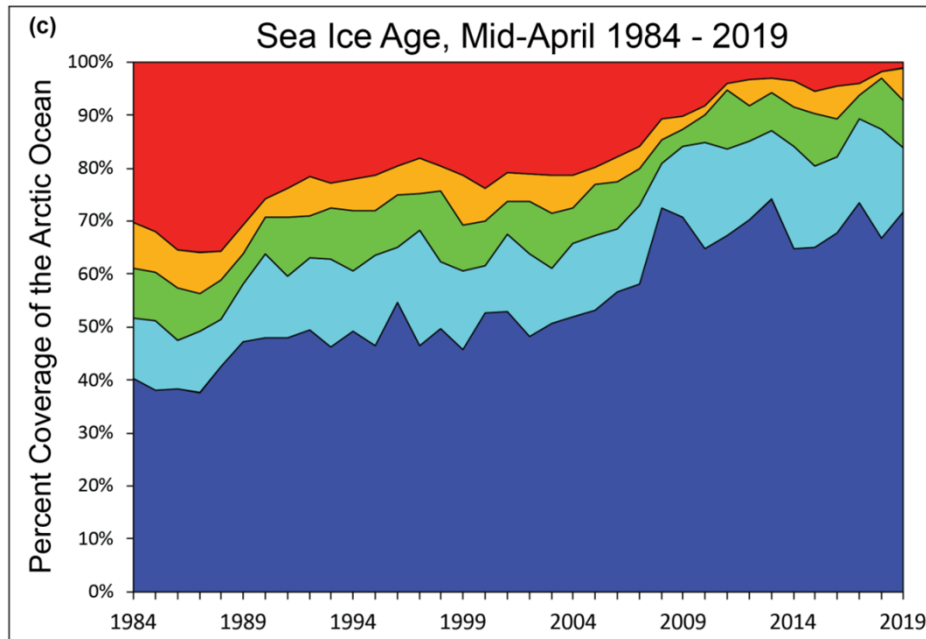
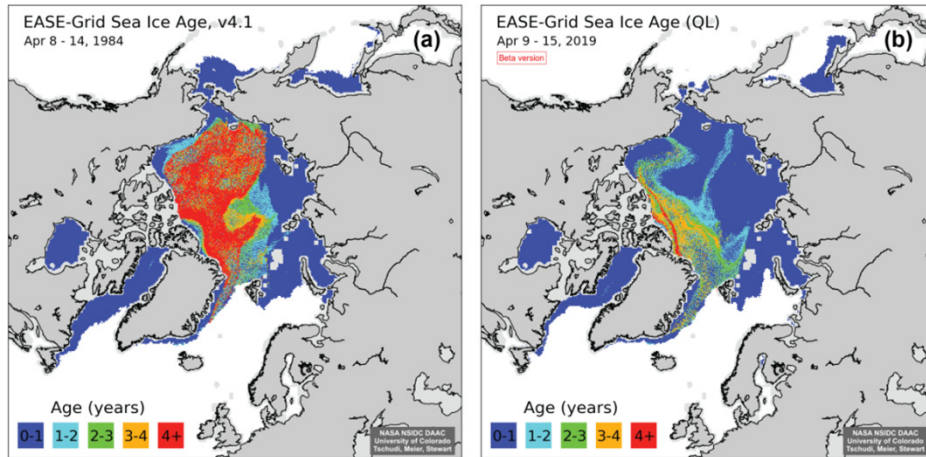
**A study of the Atlantic and Pacific waters impact  
on reduction of the Arctic sea ice**

**E.Golubeva, D.lakshina**



Russian Academy of Science, Siberian Branch  
Institute of Computational Mathematics and Mathematical Geophysics  
Novosibirsk State University

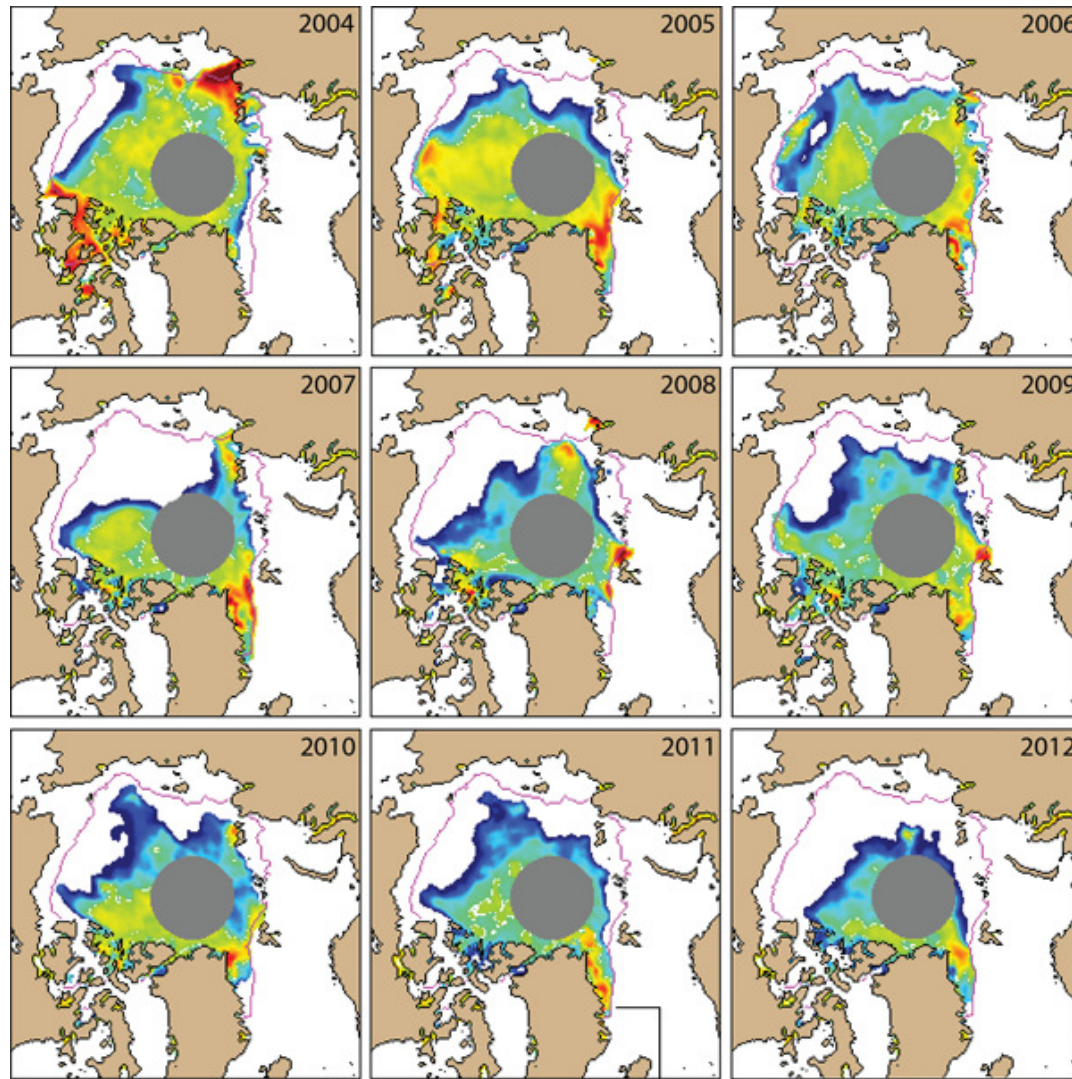
## Arctic Sea Ice Age Maps Comparing April 1984 to 2019



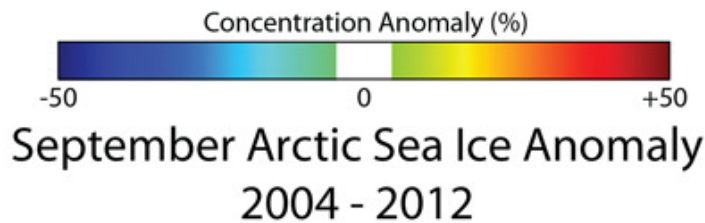
The top maps compare Arctic sea ice age for (a) April 8 to 14, 1984, and (b) April 9 to 15, 2019. The time series (c) of mid-April sea ice age as a percentage of Arctic Ocean coverage from 1984 to 2019 shows the nearly complete loss of 4+ year old ice; note that that age time series is for ice within the Arctic Ocean and does not include peripheral regions where only first-year (0 to 1 year old) ice occurs, such as the Bering Sea, Baffin Bay, Hudson Bay, and the Sea of Okhotsk.

Credit: W. Meier, NSIDC

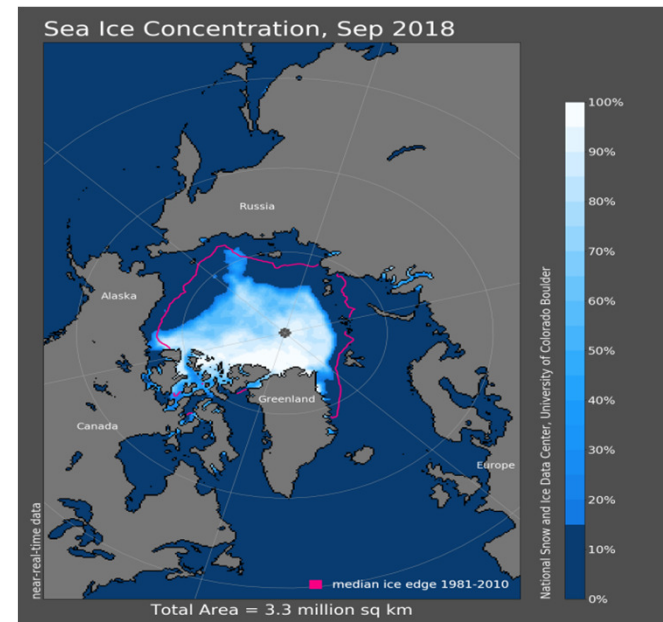
<https://nsidc.org/arcticseaicenews/>



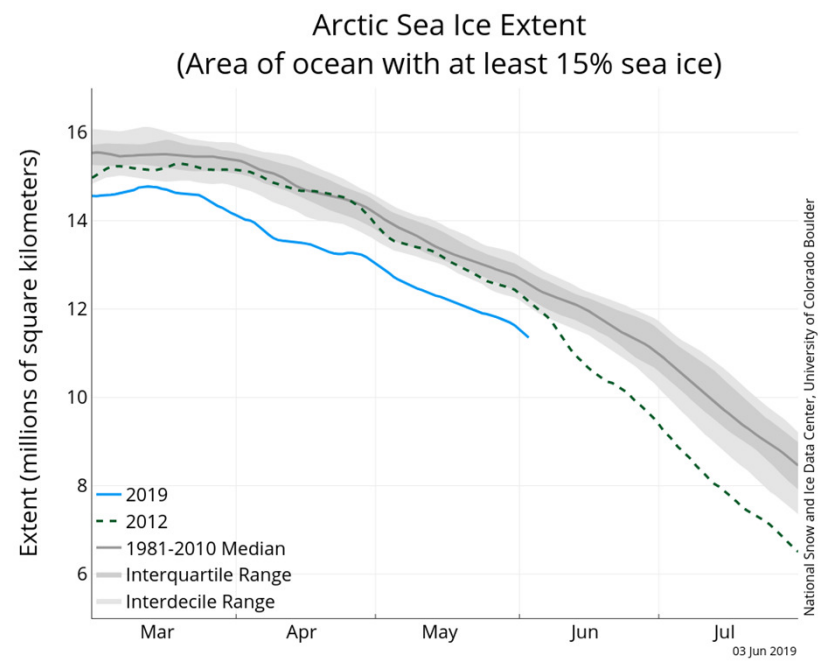
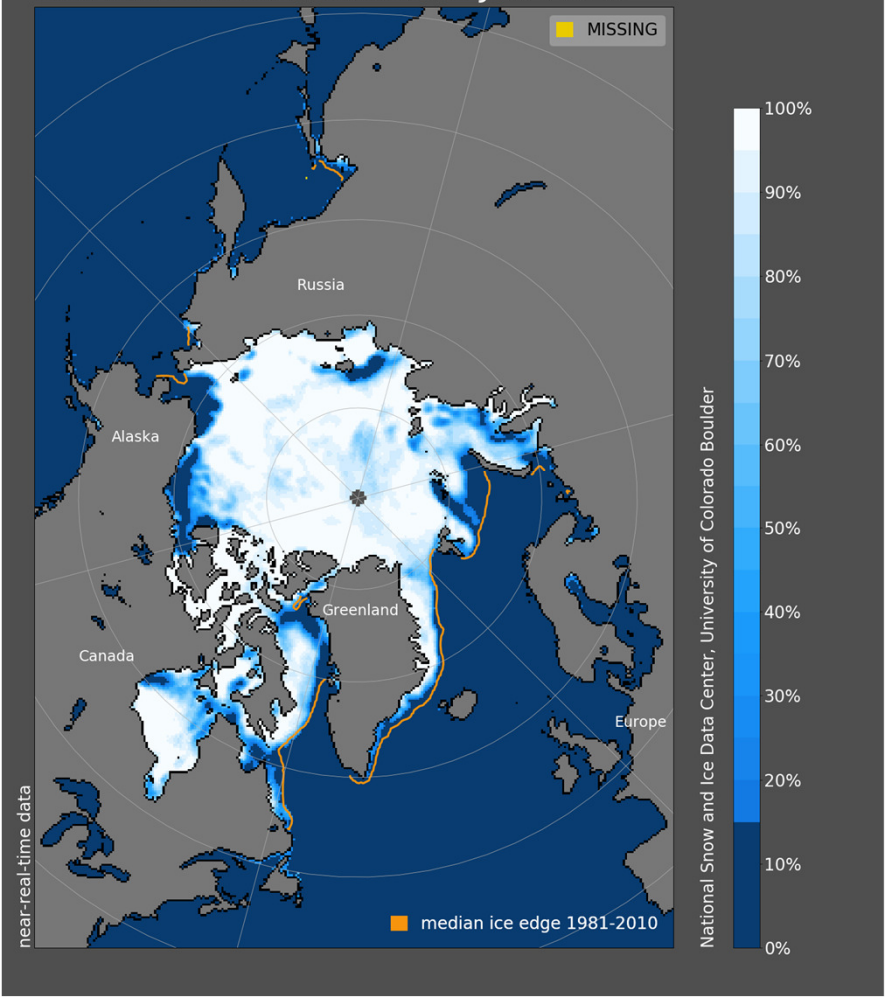
September 1979-2000  
Median Extent



According to the NSIDS data, the absolute minimum of the sea ice area in the Arctic is 3.41 million square kilometers (September 2012), which is 49% lower than the average for the period from 1979 to 2000.



# Sea Ice Concentration, 03 Jun 2019



## MAIN REASONS FOR the ARCTIC SEA DECLINE

### Atmosphere:

Significant increase in surface air temperature in the Arctic at the end of the 20th – beginning of the 21st centuries. (AARI, Review, 2014).

Changes in the circulation regime leading to the redistribution of floating ice in the Arctic basin and the formation of sustainable ice removal beyond its limits. (Ivanov et al., 2013)

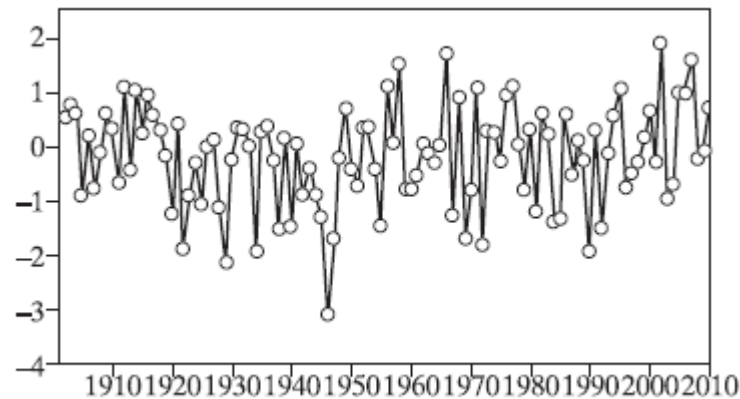
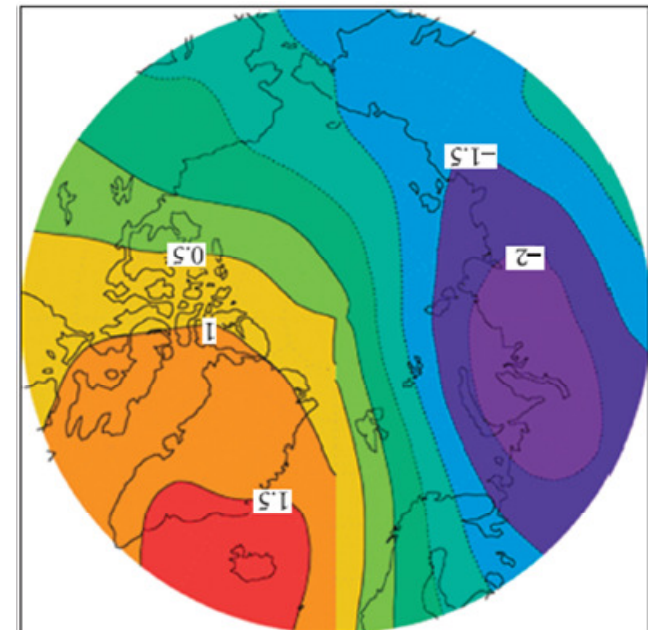
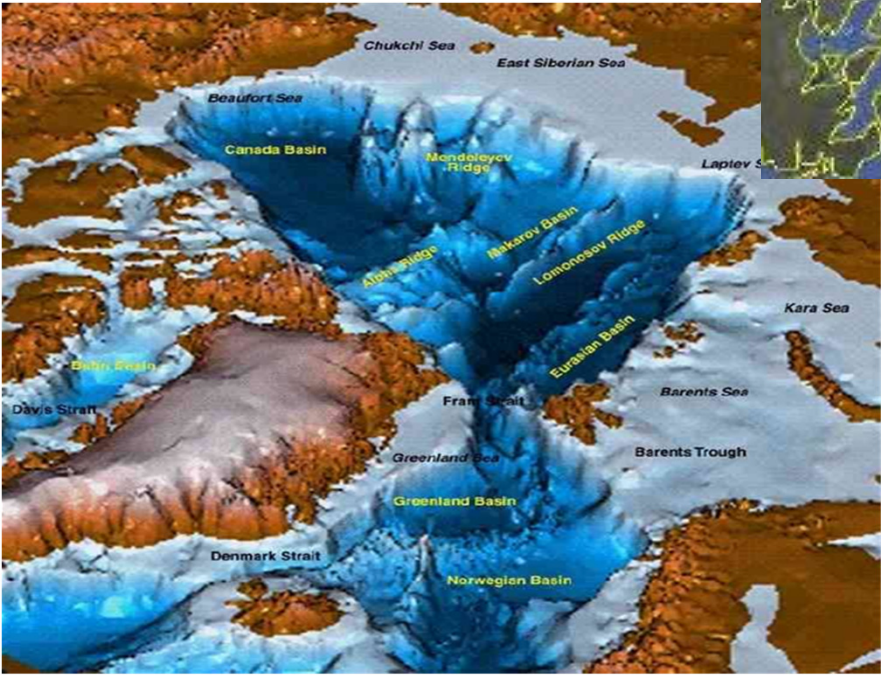
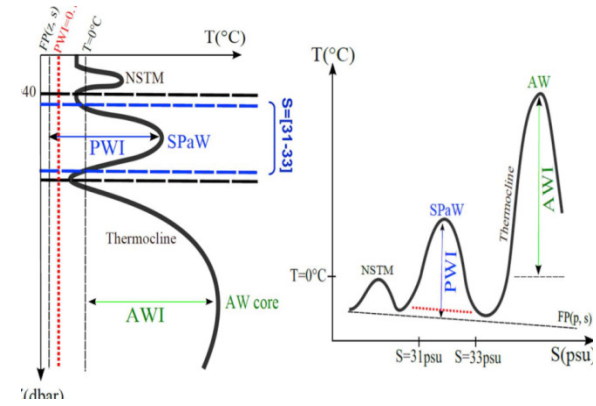
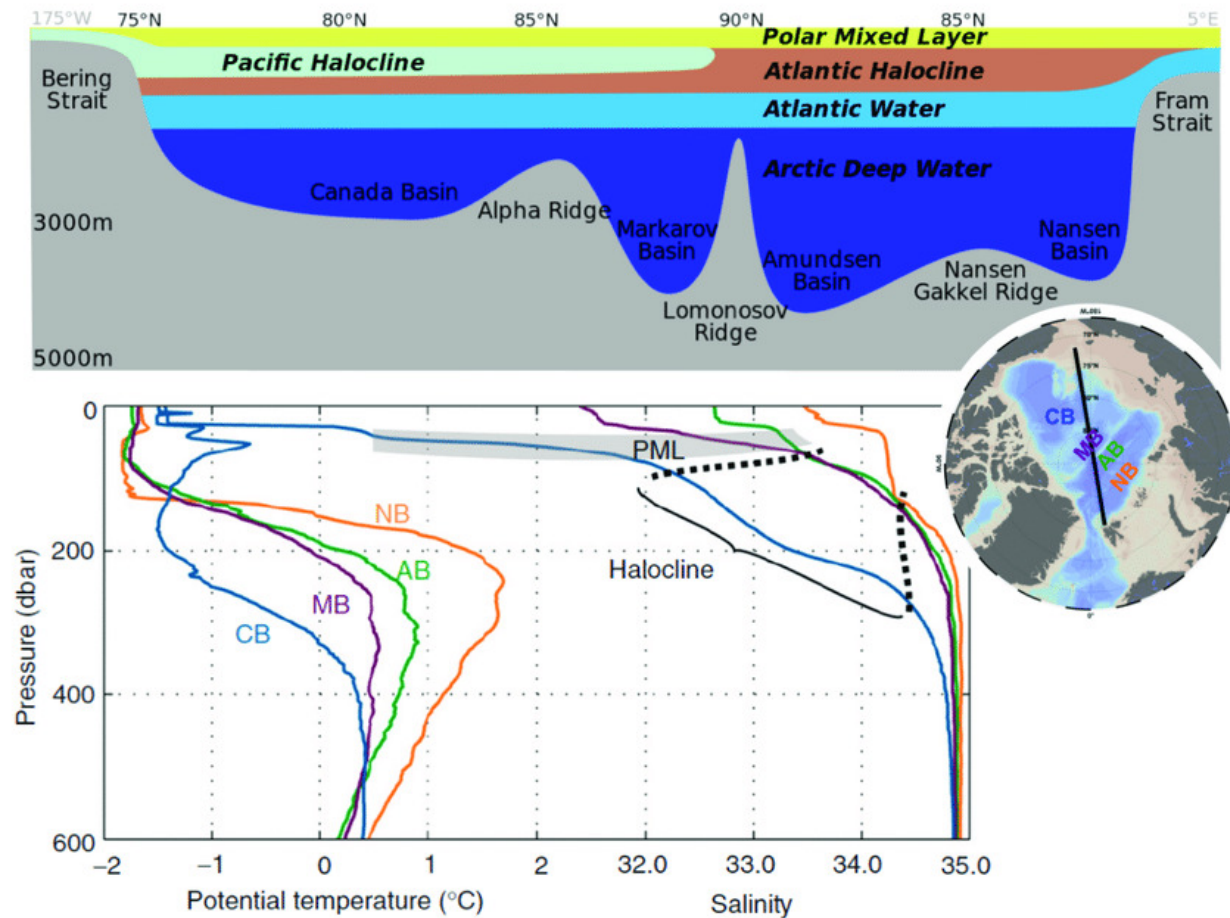


Рис. 6. Распределение аномалий приземного давления, соответствующих моде, обеспечивающей усиление Трансдрифта (а), и временной ряд коэффициента Фурье этой моды с 1900 г. (б).





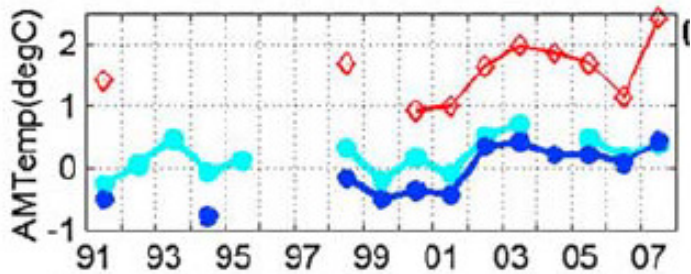
Hydrography of the Arctic Ocean. Schematic vertical distribution of the major water masses in the Arctic Ocean based on a hypothetical transect from 175°W to 5°E (black line in the map) [Aagaard and Carmack, 1989]. Typical vertical distribution of potential temperature (°C) and salinity for Nansen Basin (NB), Amundsen Basin (AB), Markarov Basin (MB) and Canada (CB). PML indicates Polar Mixed Layer [Rudels, 2009]



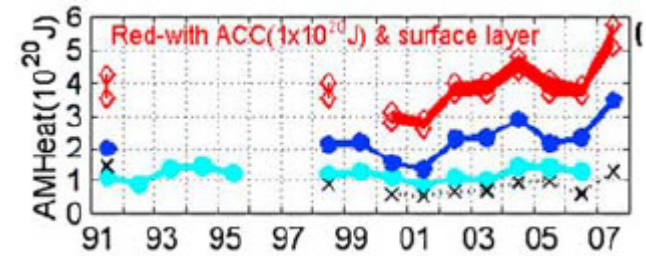
Aagaard, K., and E. C. Carmack (1989), The role of sea ice and other fresh water in the Arctic circulation, *J. Geophys. Res.*, 94(C10), 14485, doi:10.1029/JC094iC10p14485.

Rudels, B. (2009), Arctic Ocean Circulation, in *Ocean Currents: A Derivative of the Encyclopedia of Ocean Sciences*, edited by J. H. Steele, S. A. Thorpe, and K. K. Turekian, pp. 211–225

Pascaline Bourgain and Jean Claude Gascard, *GEOPHYSICAL RESEARCH LETTERS*, VOL. 39, L05603, doi:10.1029/2012GL051045, 2012



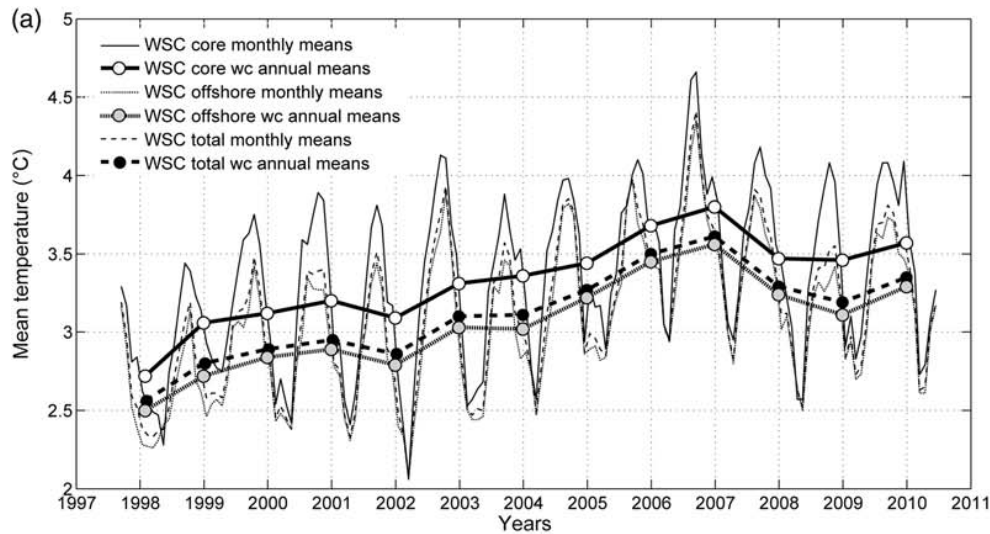
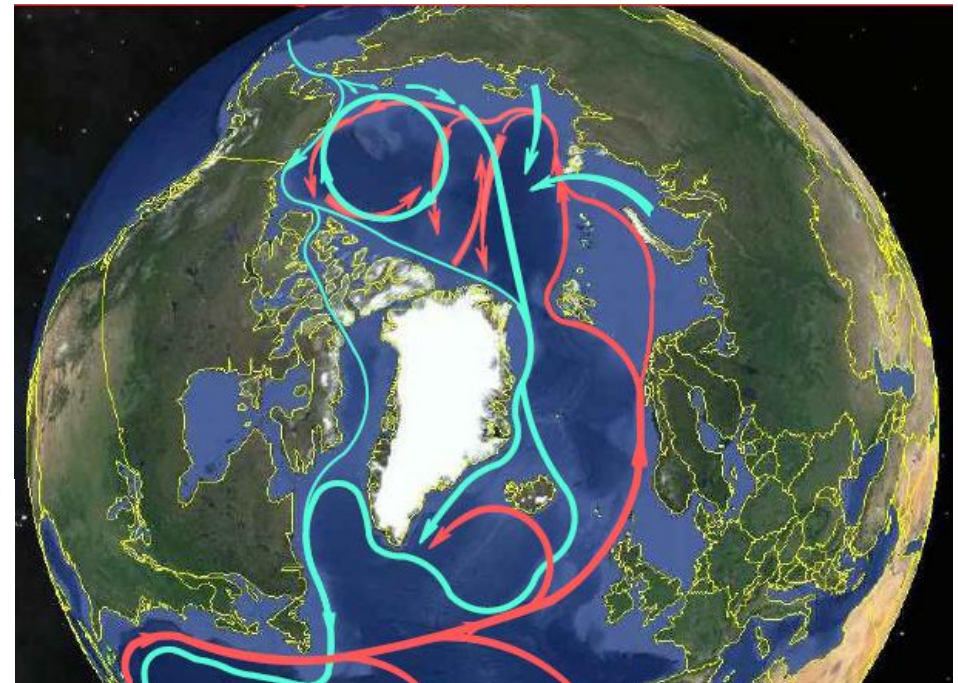
2007-5-5.7 e+20 J/yr.  
 2004-4.3-4.8 e+20 J/yr  
 2001-2.6-2.9 e+20 J/yr



*R.Woodgate et.al.,2010*

## Ocean:

increased thermal effects from  
 Atlantic and Pacific waters  
 entering the Arctic basin

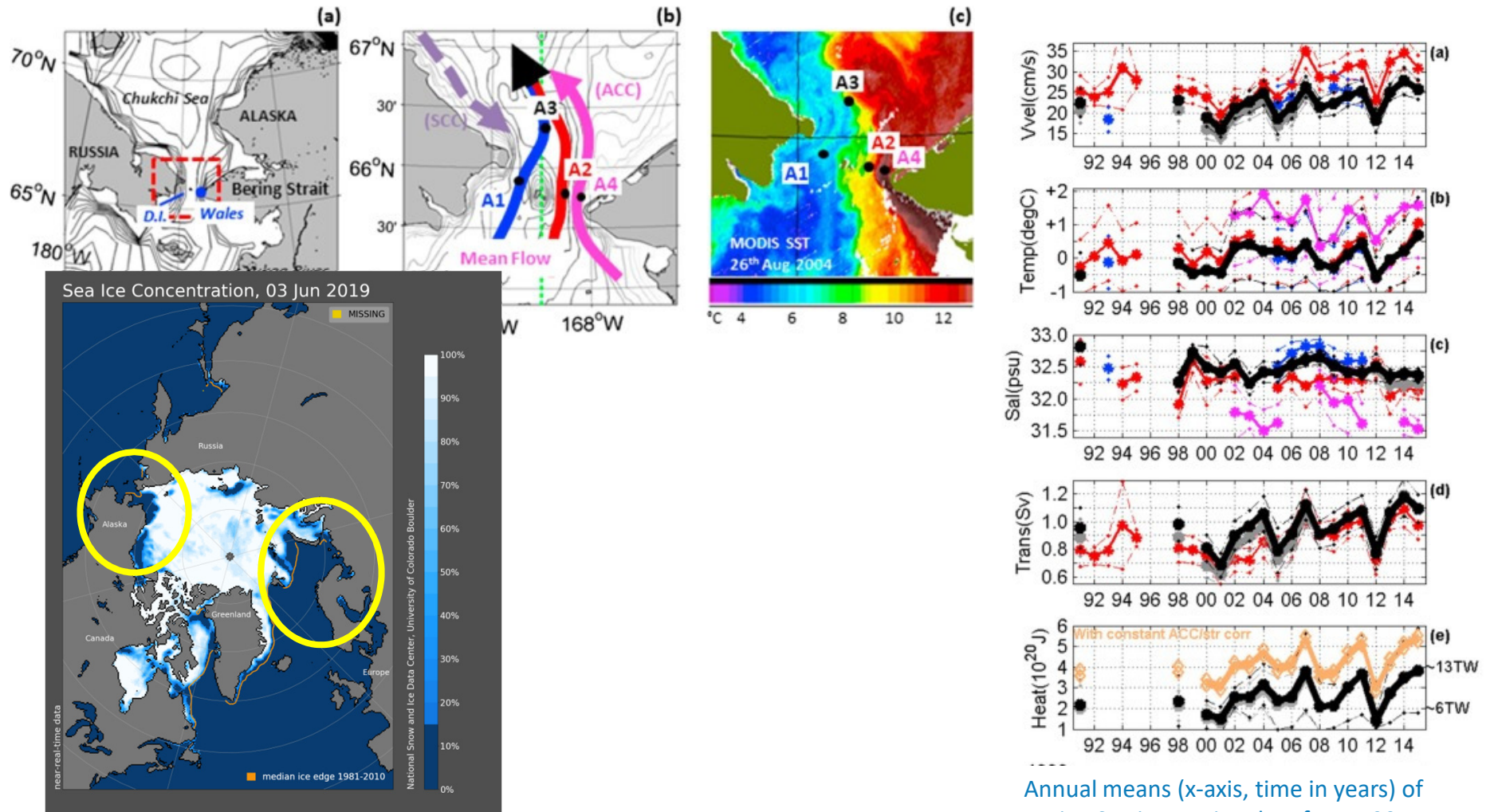


*A.Beszczyńska-Møller et. al.,2012*

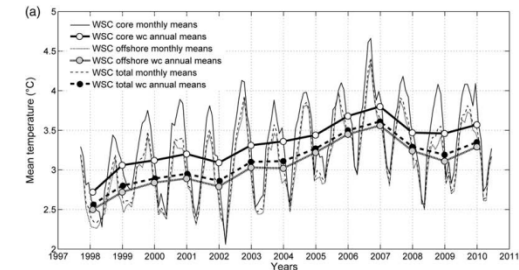
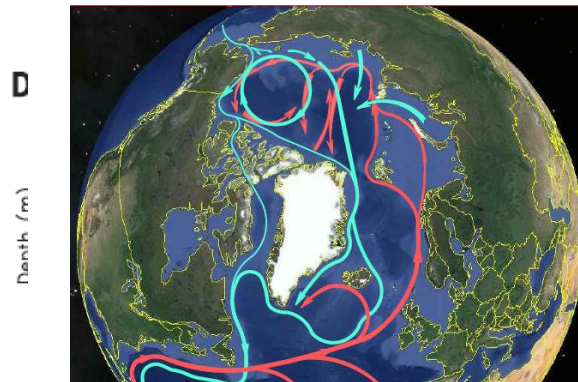
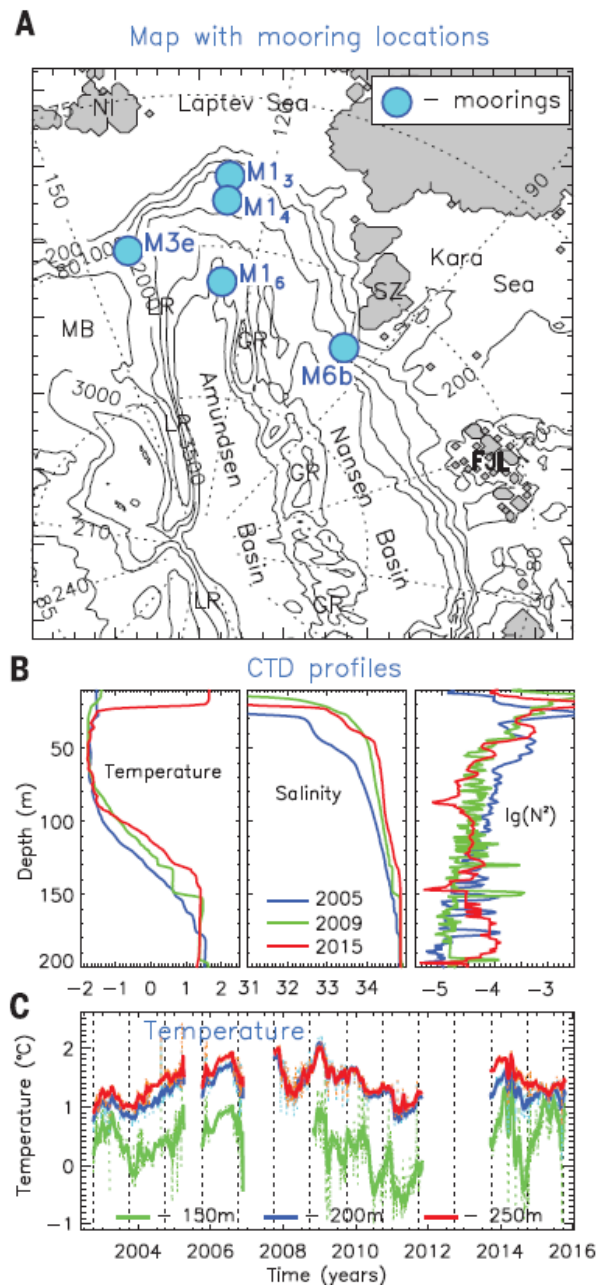


Rebecca A. Woodgate, <https://doi.org/10.1016/j.pocean.2017.12.007>

## Increases in the Pacific inflow to the Arctic from 1990 to 2015, and insights into seasonal trends and driving mechanisms from year-round Bering Strait mooring data



Annual means (x-axis, time in years) of Bering Strait mooring data from 1991 to 2015 at A1 (blue), A2 (red), A4 (magenta) and A3 (uncorrected data - grey; corrected data - black)



A.Beszczynska-Moller et al., 2012

Polyakov et al., *Science* 356, 285–291 (2017) 21 April 2017

**Fig. 2. Mooring locations and time series and their wavelet transforms from the mooring site M14, eastern EB of the Arctic Ocean.** (A) Map showing locations of oceanographic moorings. The Gakkel Ridge (GR) divides the EB into the Nansen Basin (NB) and the Amundsen Basin (AB). The Lomonosov Ridge (LR), Novosibirskiye Islands (NI), Severnaya Zemlya (SZ), Franz Joseph Land (FJL), and Makarov Basin (MB) are indicated. Dotted lines show latitudes and longitudes; gray solid lines show depth in meters. (B) Vertical profiles show increasing water temperature (°C) and salinity and decreasing stability expressed as the logarithm of squared Brunt-Väisälä frequency ( $N^2$ ,  $s^{-2}$ , a measure of water-column stability) within the cold halocline layer (CHL) and upper pycnocline (~40 to 150 m) in the 2000s and early 2010s.



SibCIOM

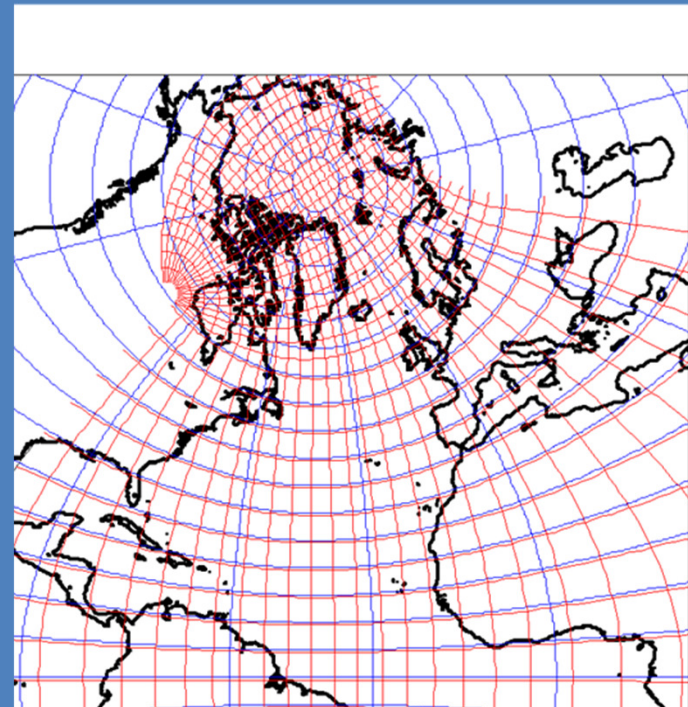


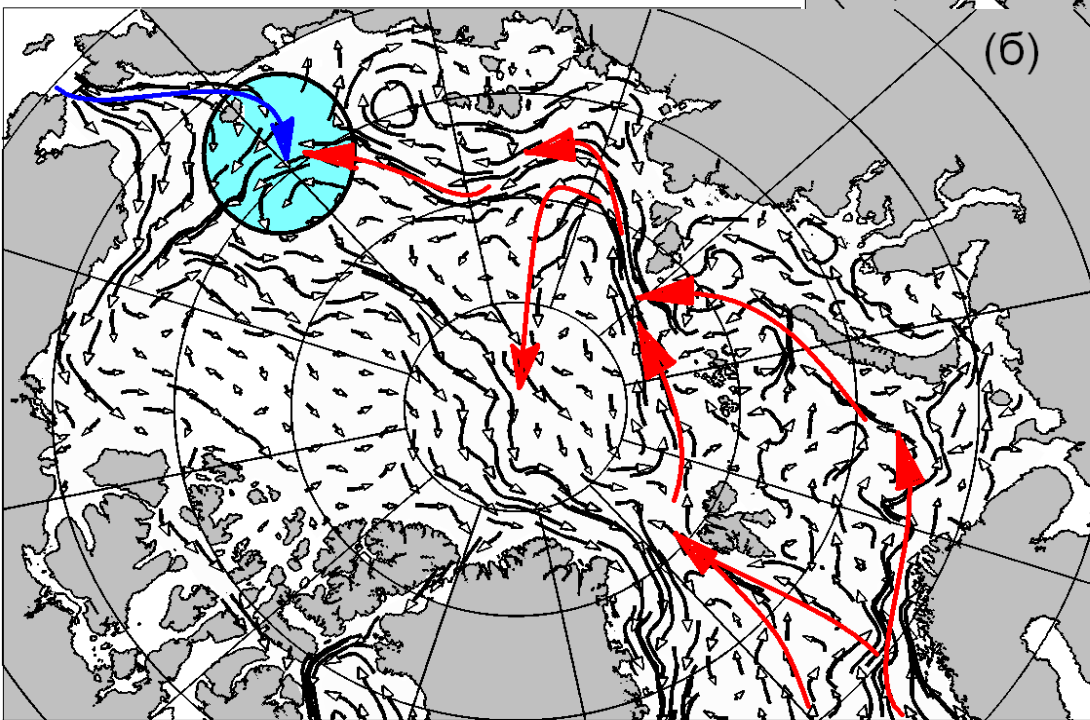
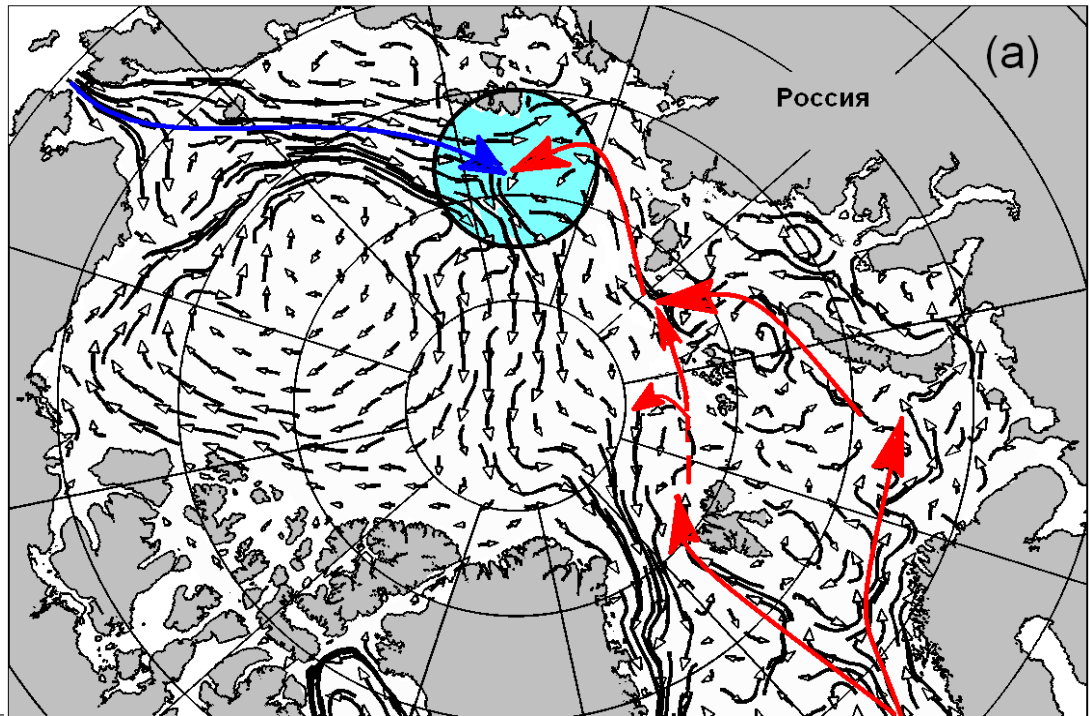
**Ocean –numerical  
model ICMMG SB  
RAS**

34-50км , and 14-19км  
38 vertical levels

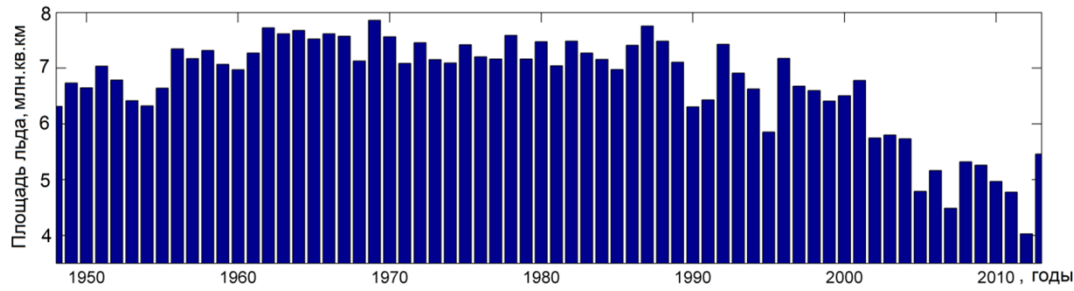
**Atmosphere-  
Reanalysis data:  
NCEP/NCAR, CORE2,.....**

**Ice-CICE 3.14**

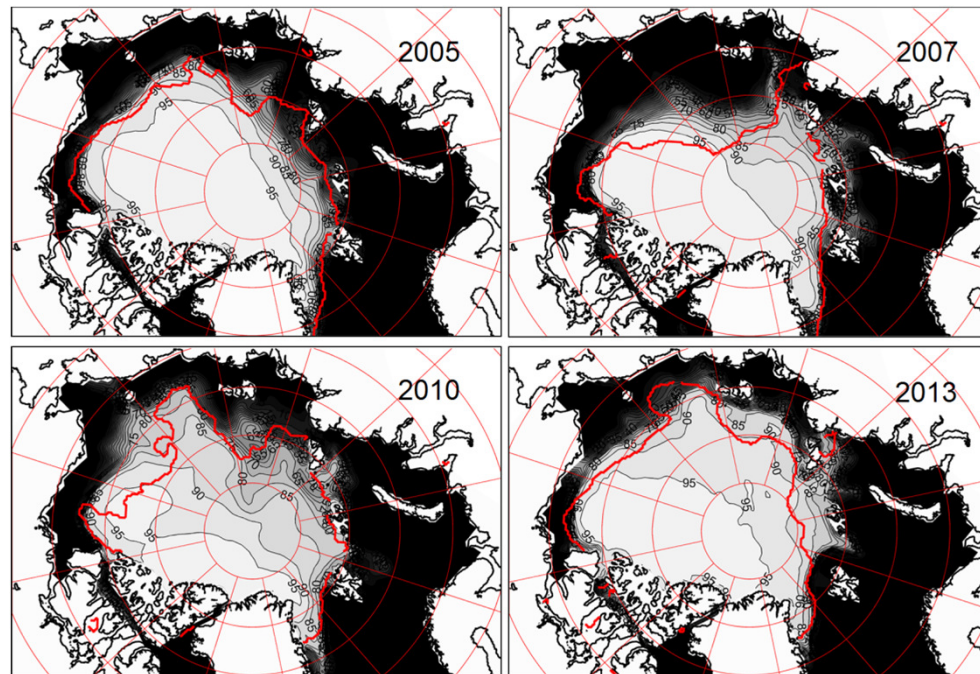




*Model currents field at a depth of 100 m: (a) – 1970 year, (b) – 1990 year.*

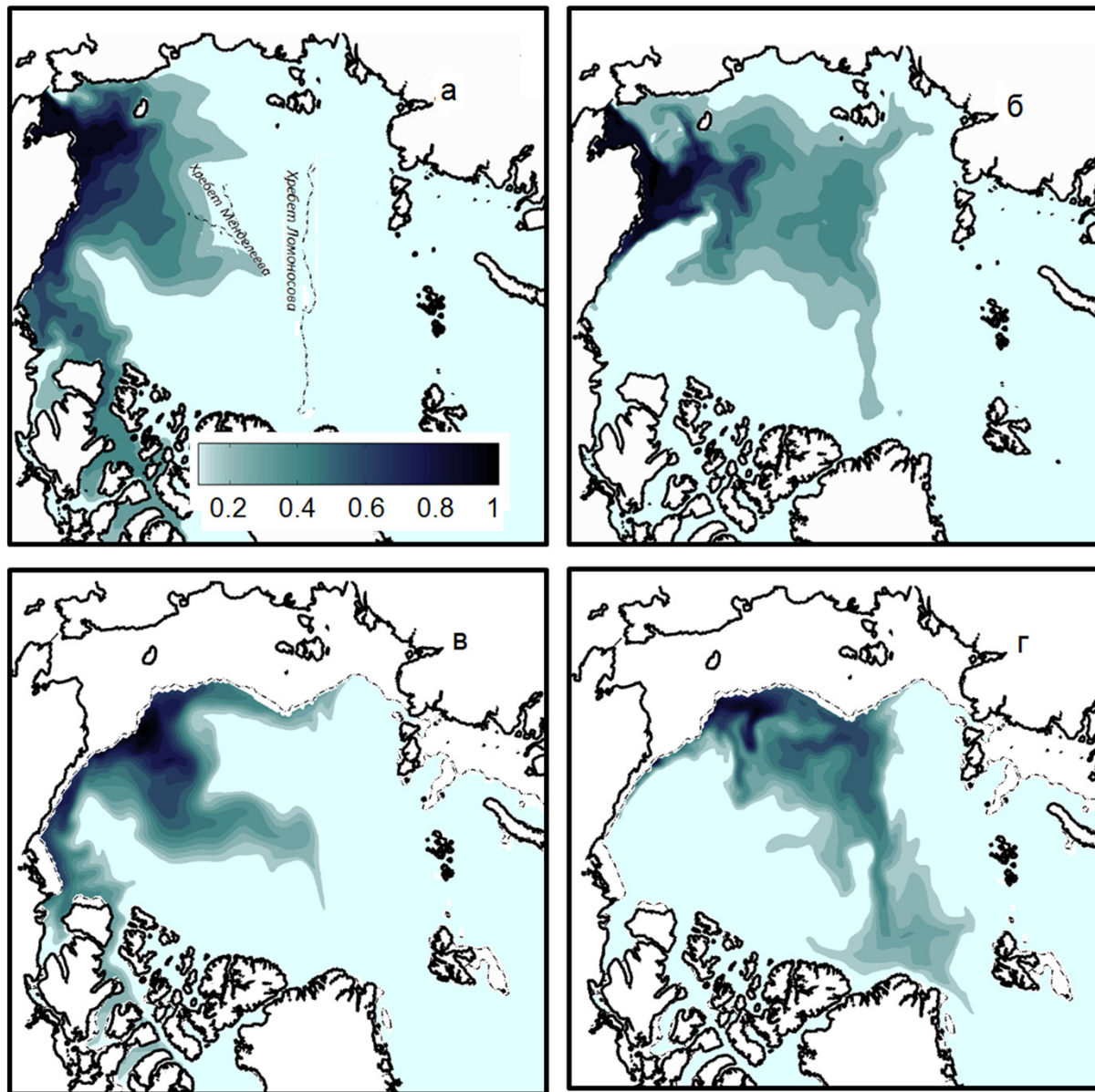


The graph above shows Arctic sea ice extent (in millions of sq km) on September based on numerical modeling

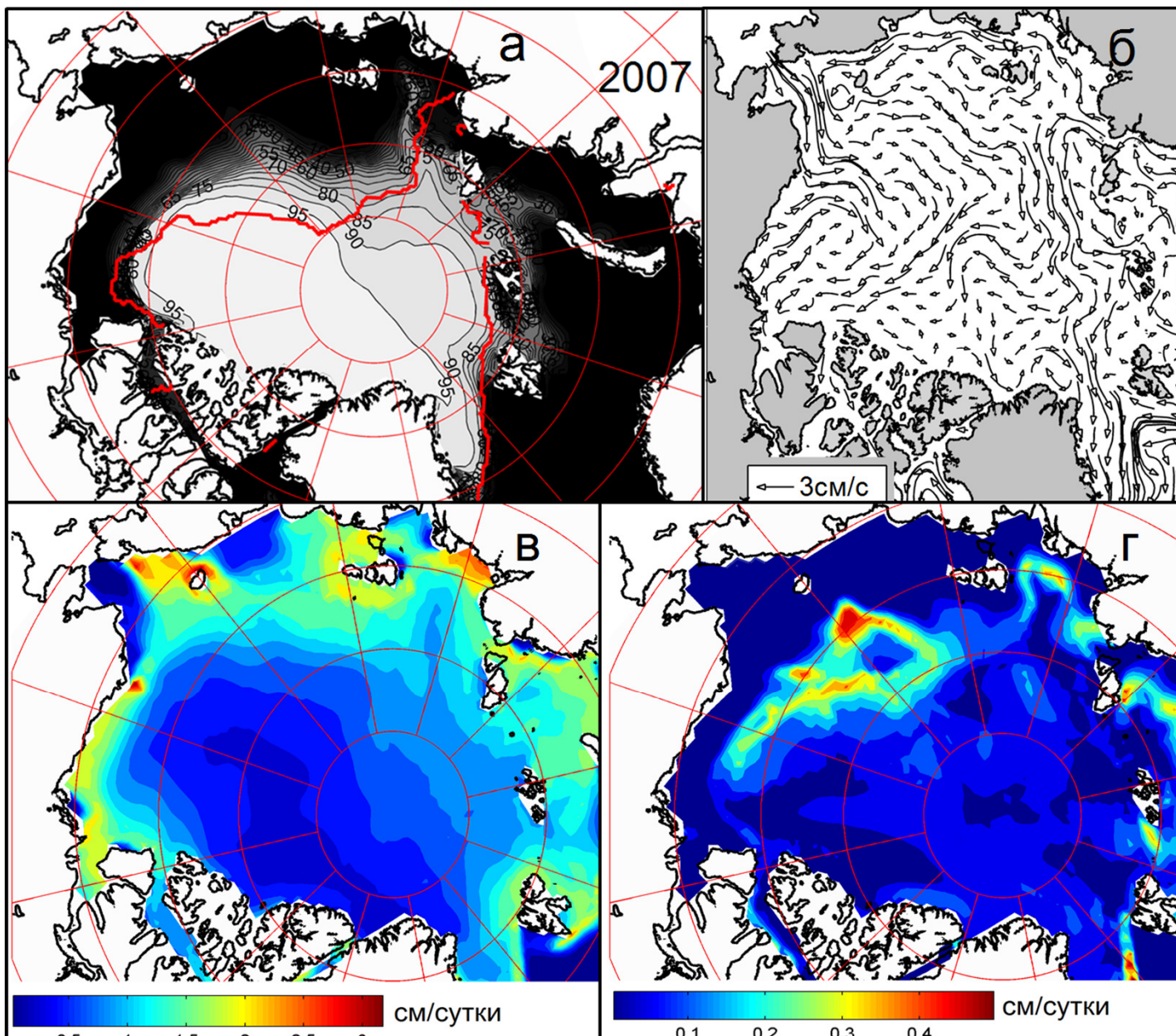


Model sea ice state in summer. September Sea-ice concentration (in percents). The red line presents the observed ice edge position (15%) derived from NSIDC data

Concentration of Pacific water tracer in 1989-1995 (a,b) and in 2000-2009 (б,r). Upper panels show tracer concentration at the sea surface, lower panels – at the depth of 100 m.



Model sea ice state in summer, 2007. September Sea-ice concentration (in percents). The red line presents the observed ice edge position (15%) derived from NSIDC data (a); averaged velocity in the upper 150m layer (б); ice melting rate in July (в) and in September (г)

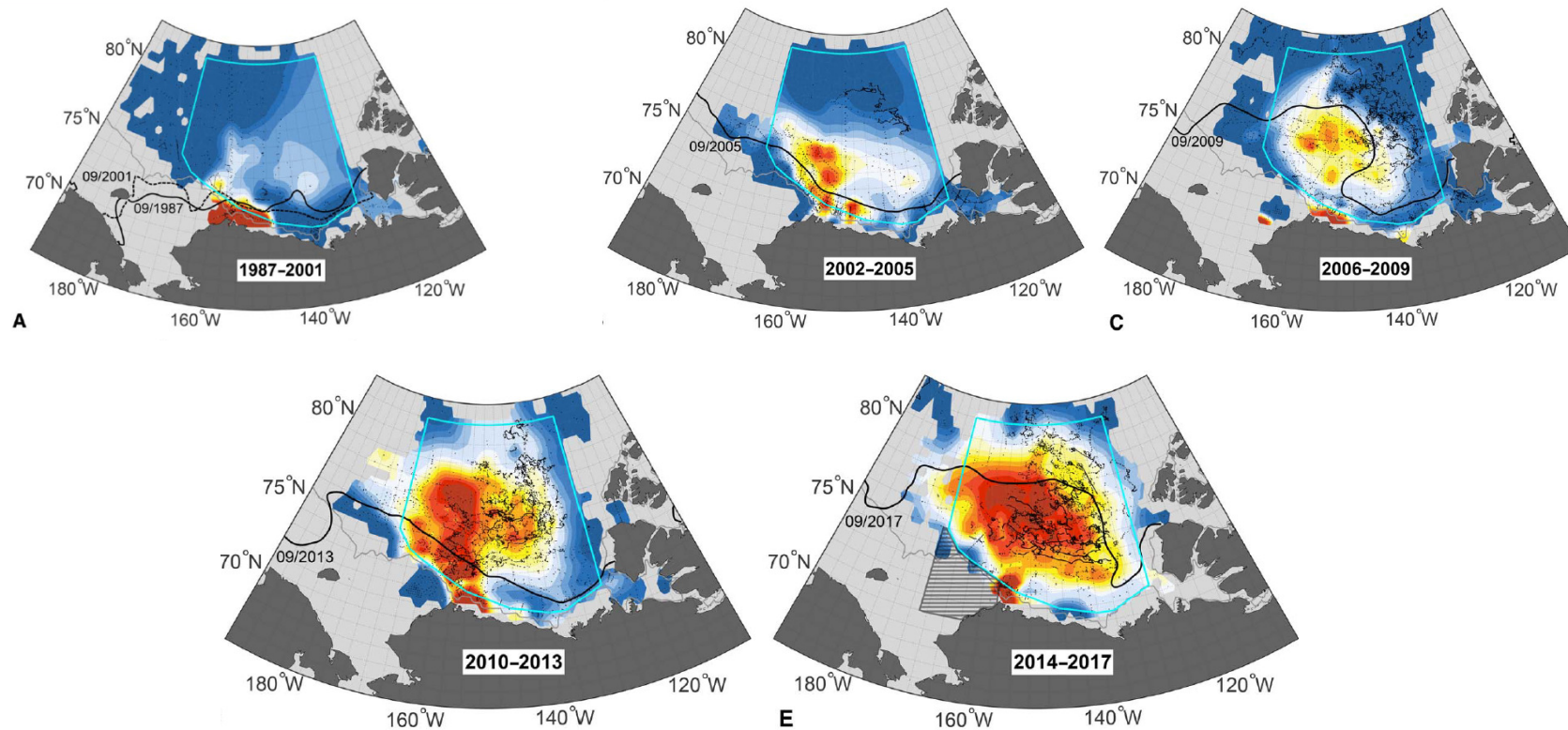


# Warming of the interior Arctic Ocean linked to sea ice losses at the basin margins

Mary-Louise Timmermans<sup>1\*</sup>, John Toole<sup>2</sup>, Richard Krishfield<sup>2</sup>

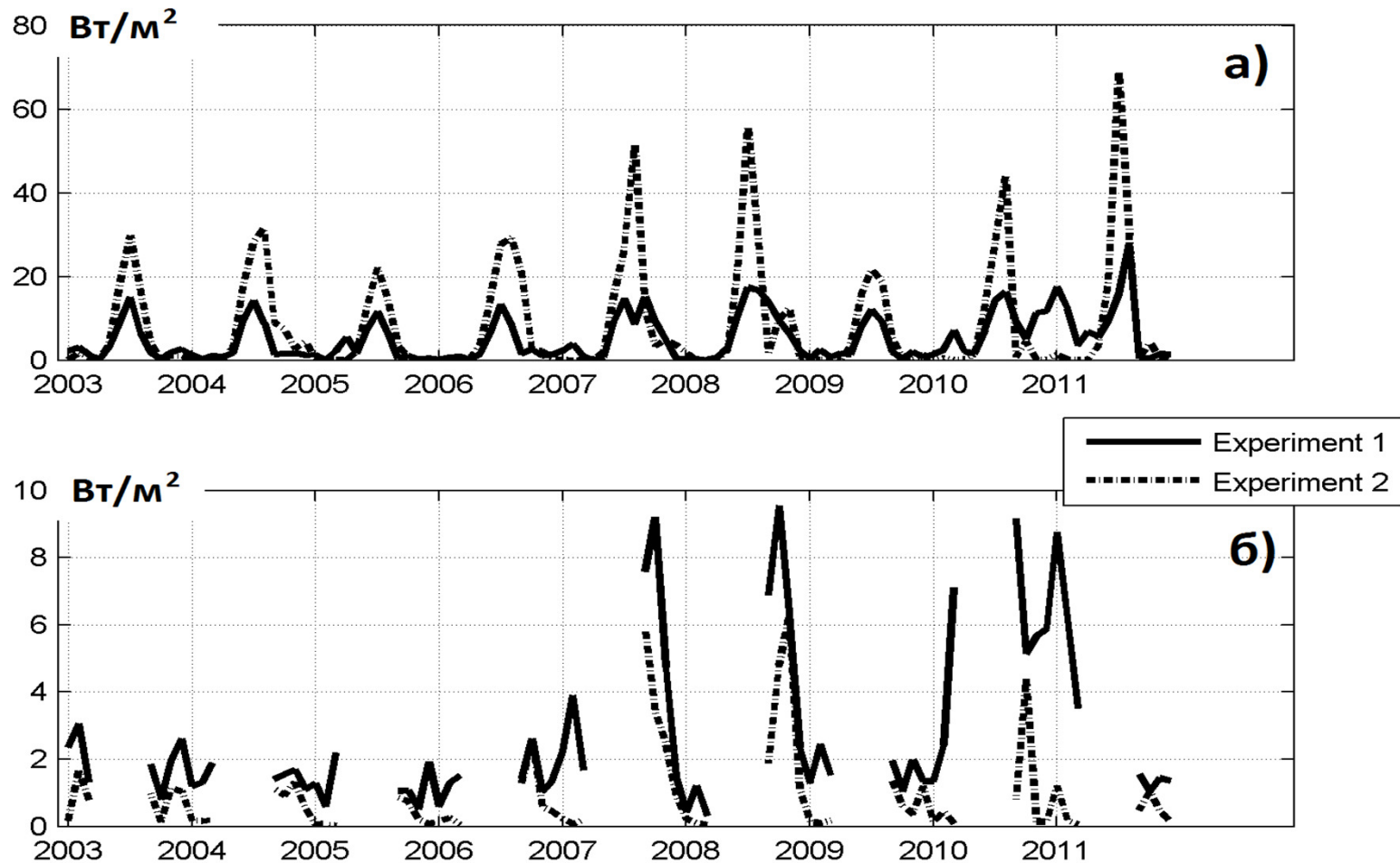
Timmermans *et al.*, *Sci. Adv.* 2018;4:eaat6773 29 August 2018

**“Arctic Ocean measurements reveal a near doubling of ocean content relative to the freezing temperature in the Beaufort Gyre halocline over past three decades (1987-2017).”**

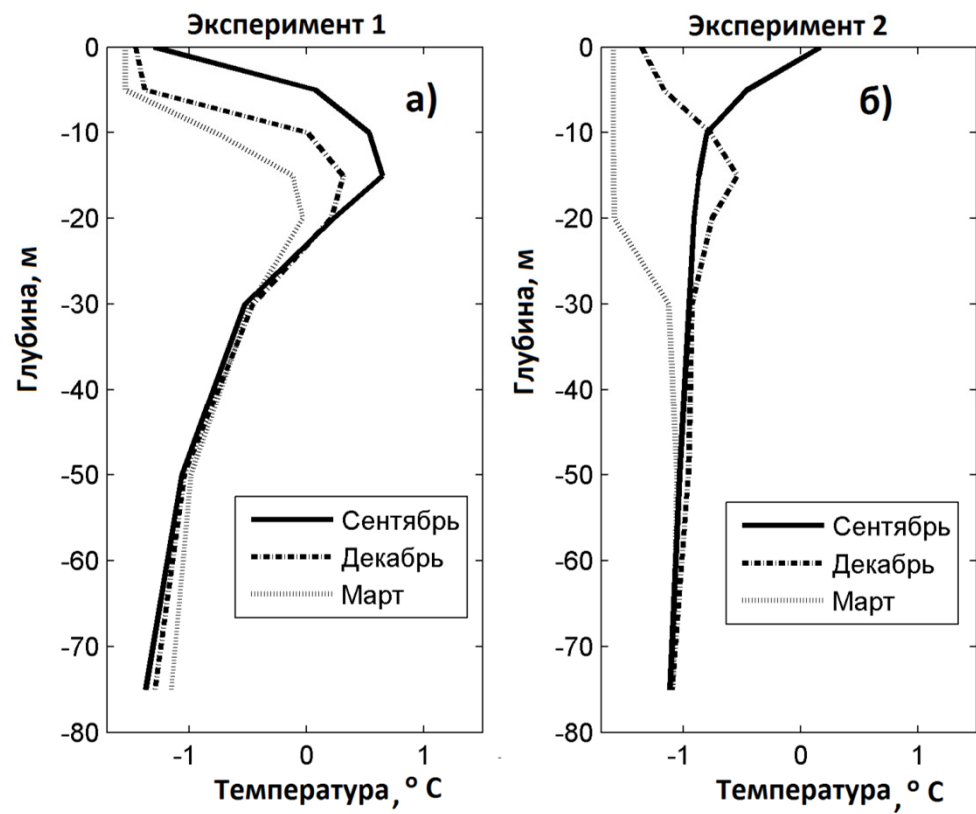


BG warm halocline . Heat content (J/m<sup>2</sup>) relative to freezing temperature integrated between isohaline S=31 and S=34

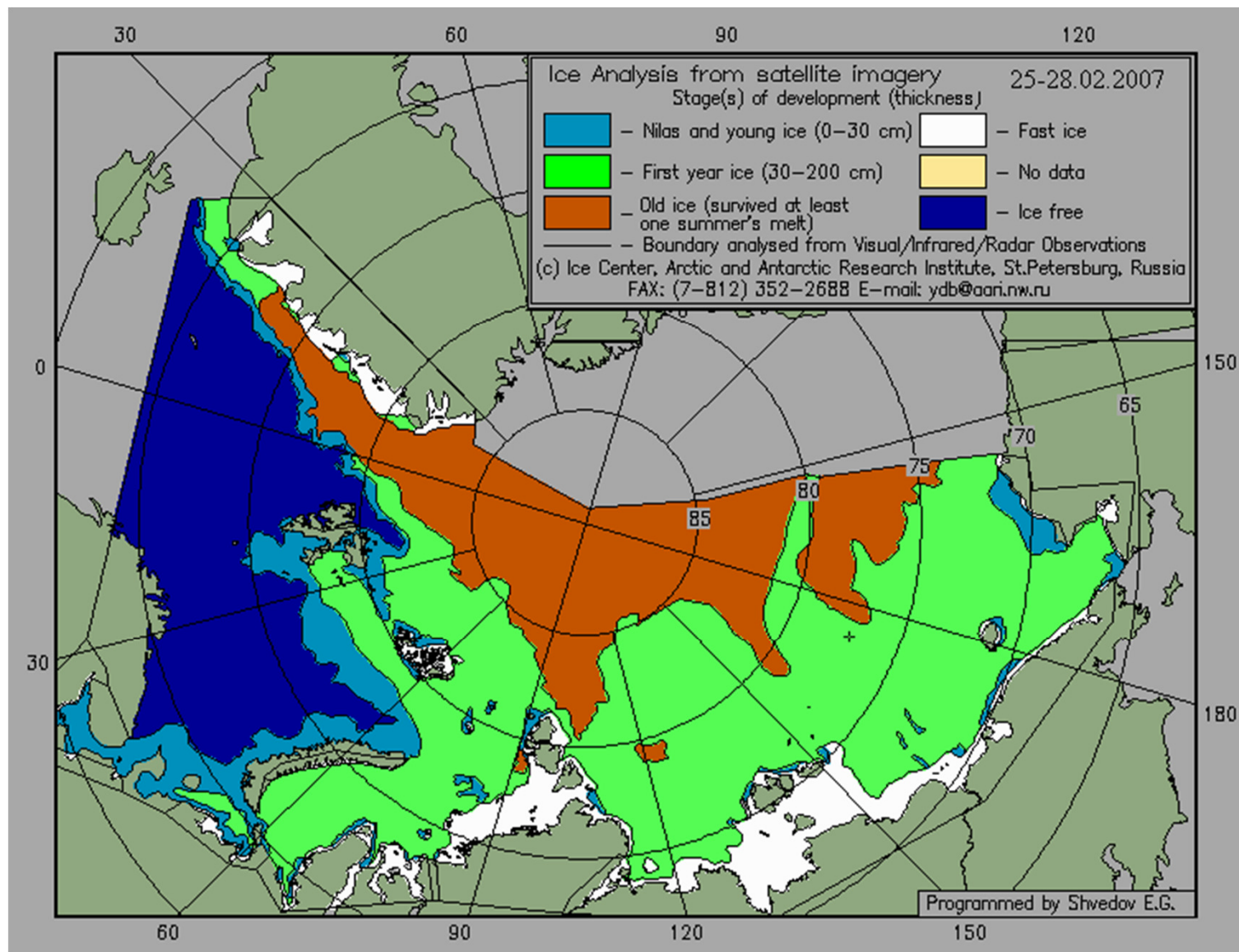


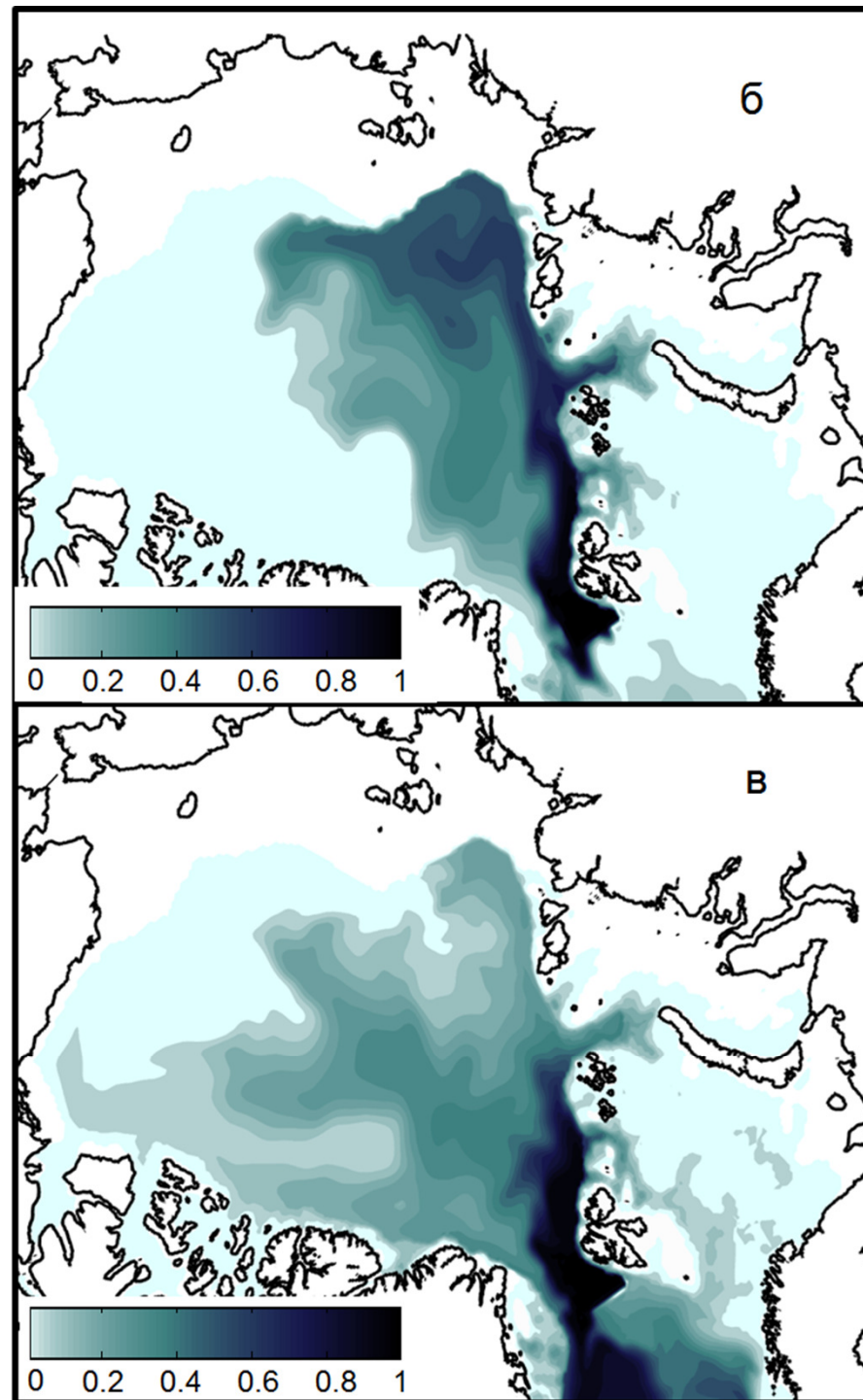
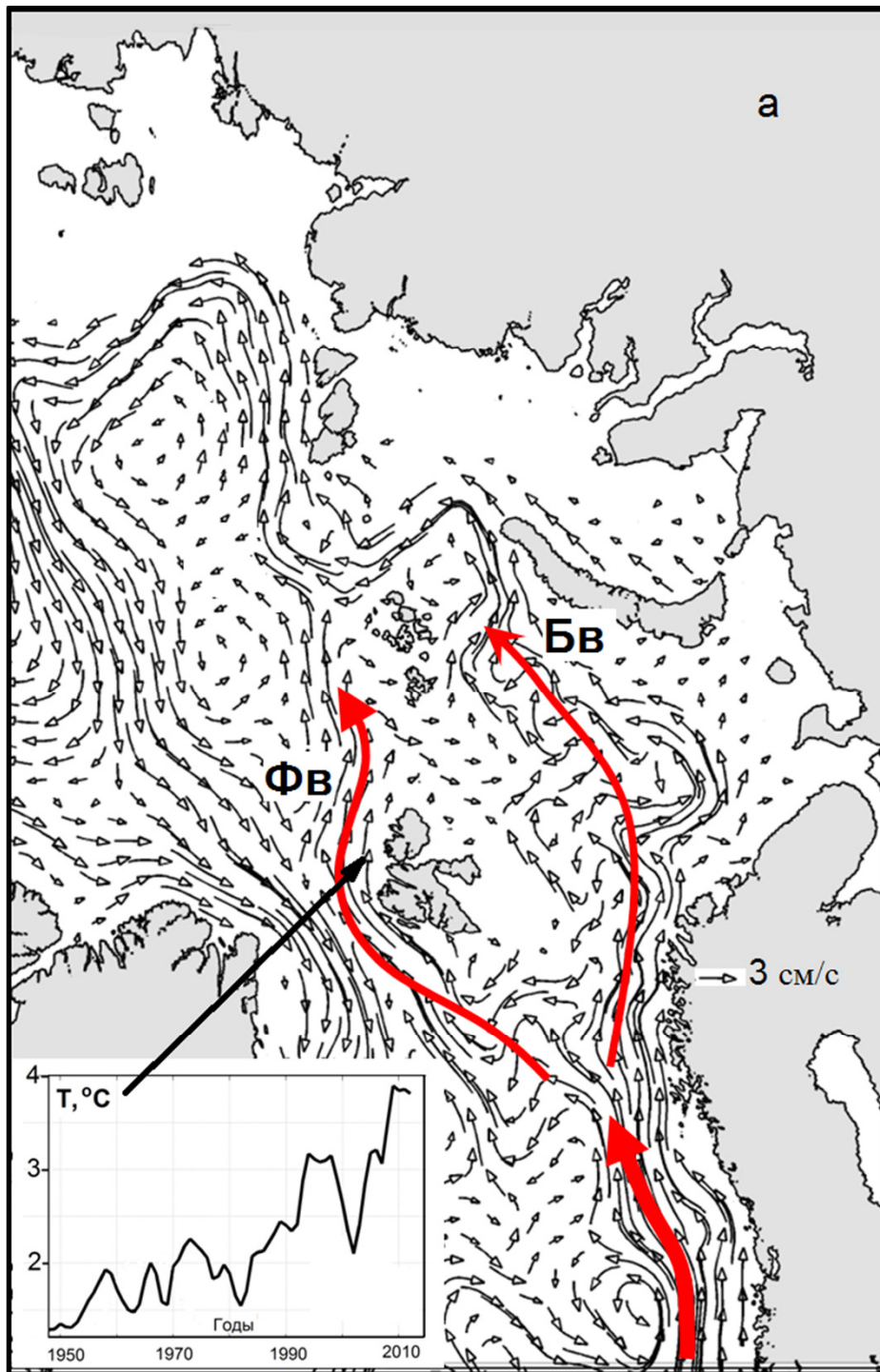


a) Heat flow from ocean to the ice ( $\text{W} / \text{m}^2$ ) in the Beaufort Sea for the period 2003-2011. The solid line is experiment 1 (taking into account penetrating radiation), the dotted line is experiment 2 (without taking into account penetrating radiation). b) Updating information for the winter months.

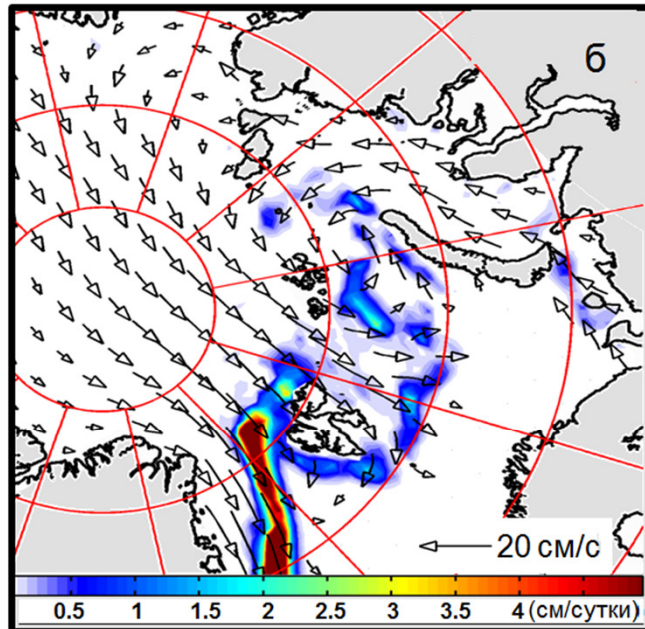
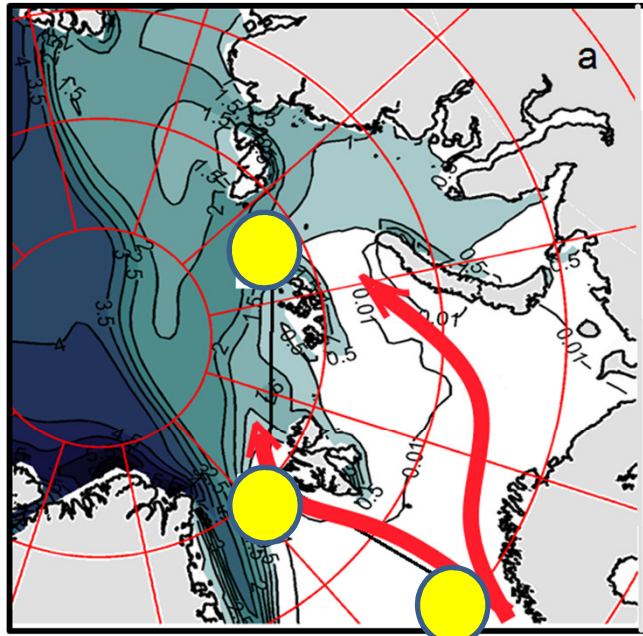


Vertical temperature profiles obtained as a result of numerical modeling for September and December 2008 and March 2009. a) Experiment 1 (taking into account penetrating radiation) b) Experiment 2 (excluding penetrating radiation)

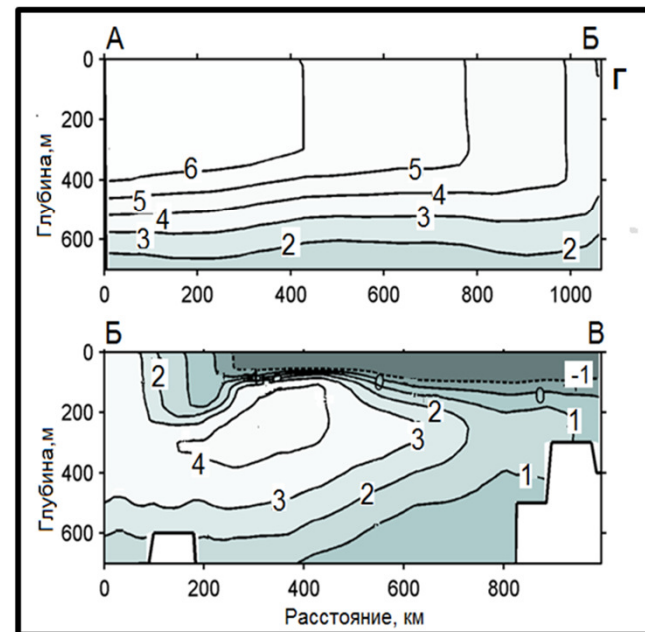
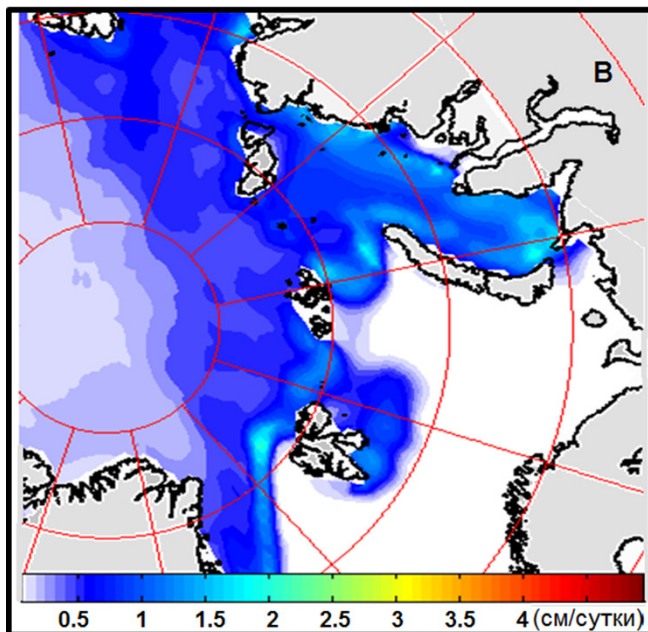




# Влияние атлантических вод на состояние ледяного покрова СЛО в численном эксперименте



Influence of Atlantic water on the Arctic sea ice in the numerical experiment. Ice thickness in February 2006 (a), ice drift and ice melting in February (б) and in July (в); temperature at the transect along Fram Strait branch of Atlantic Water in February (г)



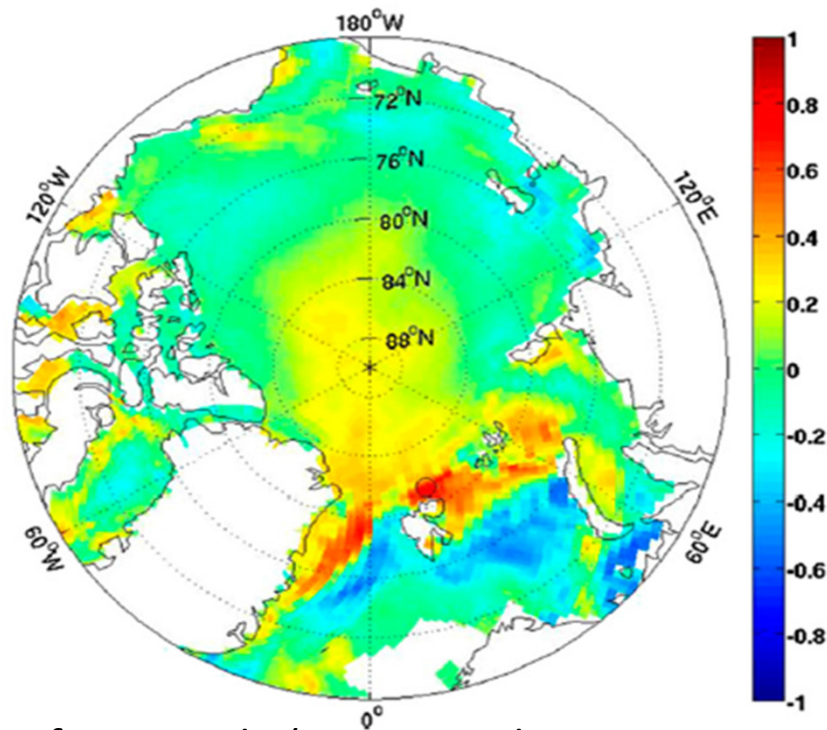
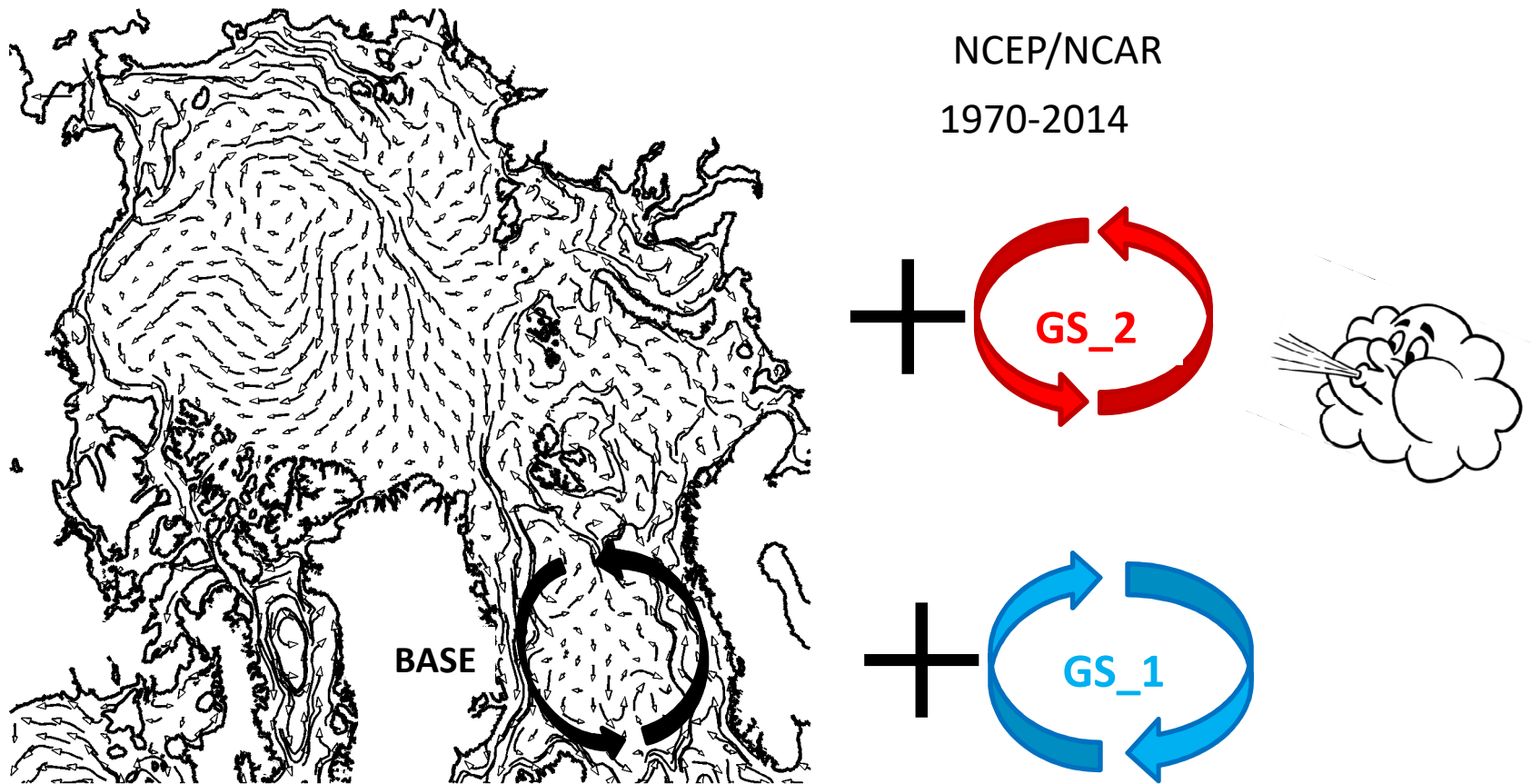
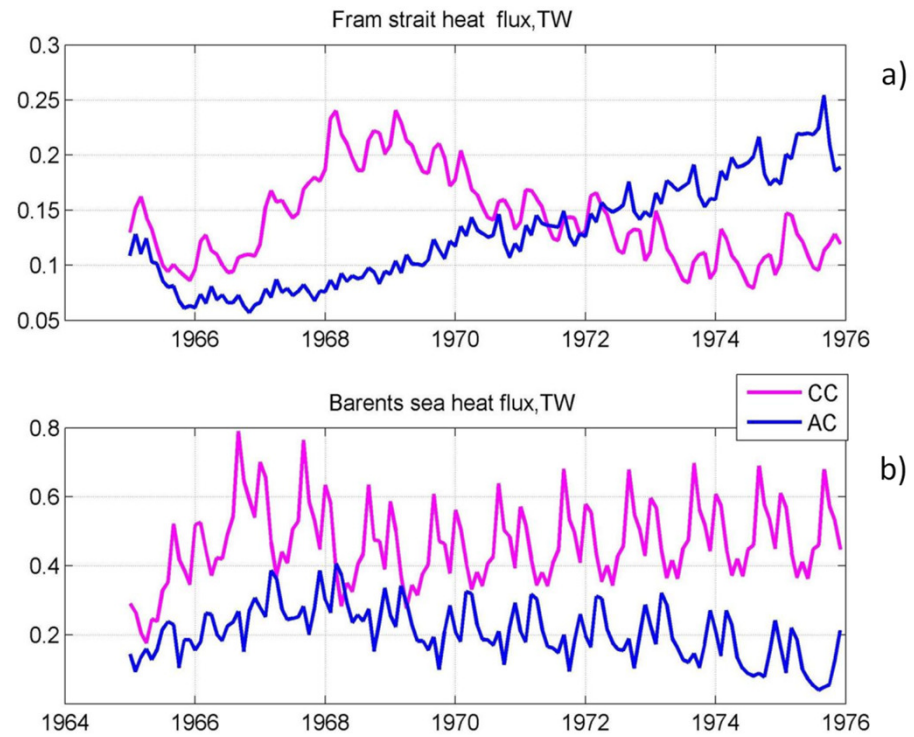


Image from article (Ivanov et al. 2016, *J. Phys. Oceanogr.*, 46, 1437-1456, DOI: 10.1175/JPO-D-15-0144.1). The spatial distribution of the correlation between the temperature in the Fram Strait at a depth of 100-200 m and the speed of ice melting at the lower boundary according to the average annual values of the period 1958-200

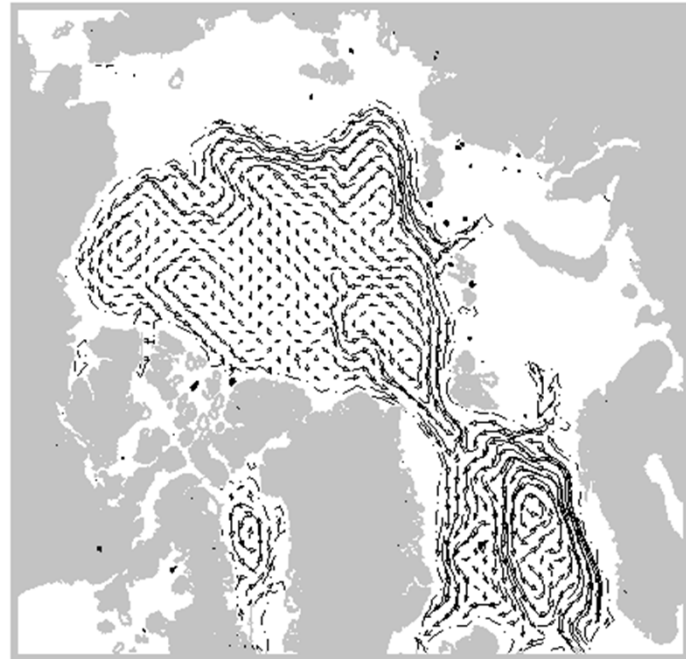
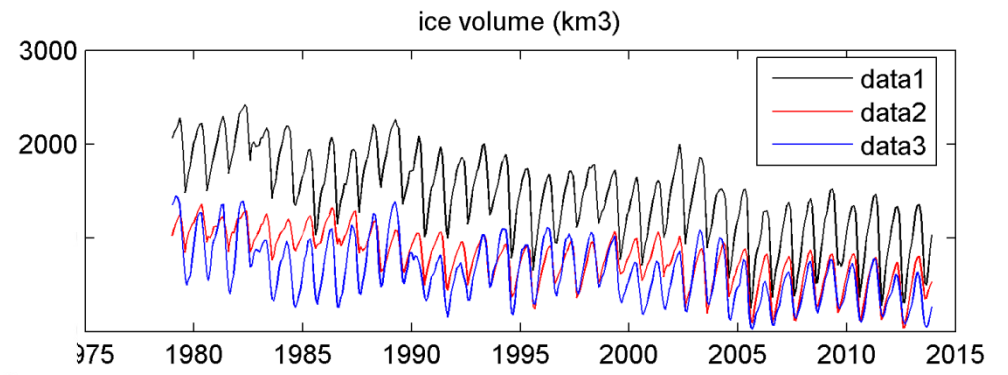
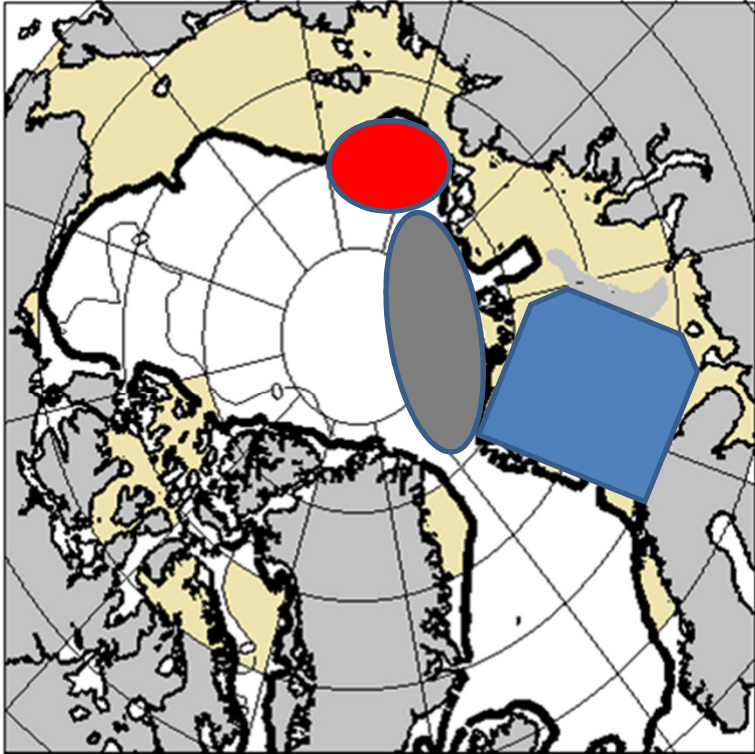
# Sensitivity study experiment





Heat flux entering the Arctic through the Fram Strait (a) and the Barents Sea (b).



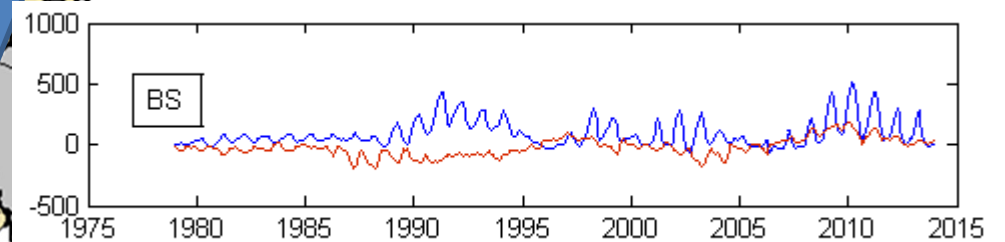
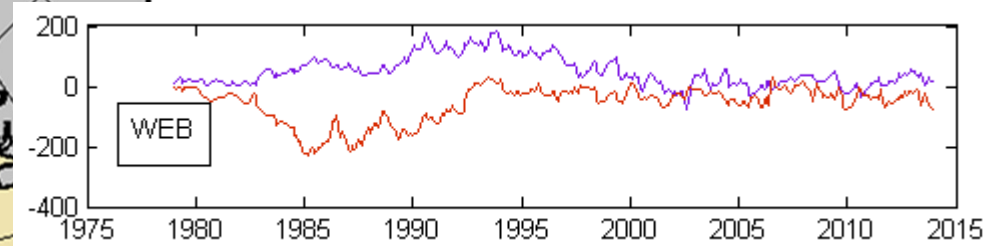
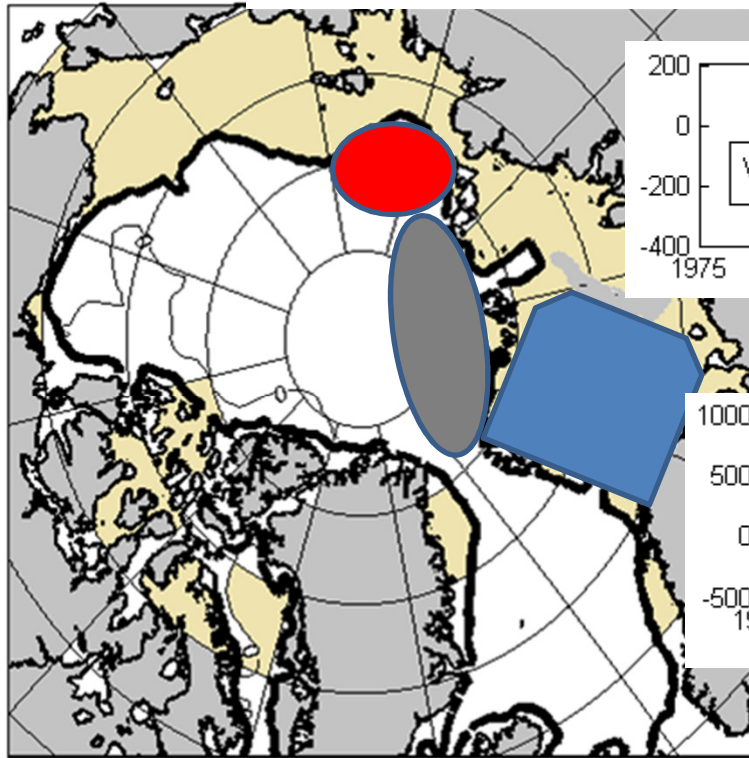
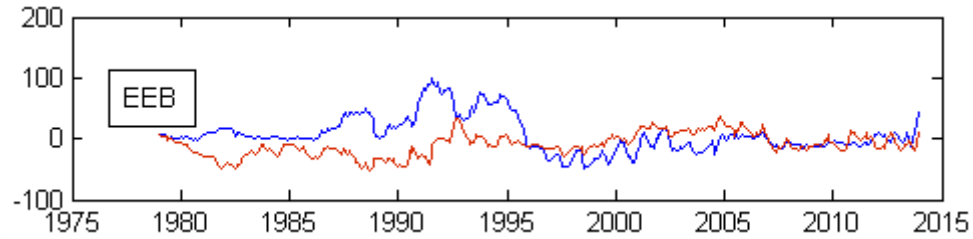




# Ice volume difference( km3)



Gs2-Base and GS\_1-Base



## **Conclusion**

Based on the simulation results, it was found that the variability of the atmospheric dynamics influences not only the sea ice, but also the trajectory of the PW and AW. Changing in the direction of AW and PW circulation is most typical for the Canadian Basin.

The areas, where the maximum melting rate at the bottom of the ice corresponds to the trajectories of the PW and AW, have been identified.

In the Atlantic region of the Arctic Ocean, the flow of warm AW causes a persistent lack of ice in the winter in the Barents Sea and in the eastern part of the Greenland Sea.

An effect of AW on the Arctic sea ice can be traced north of the Spitsbergen and along the continental slope north of the Barents Sea, where the mixing processes cause warming of overlying layers and thinning of the ice.